Percolation model of nuclear magnetic relaxation in porous media

Kenneth S. Mendelson
Physics Department, Marquette University, Milwaukee, Wisconsin 53233
(Received 24 July 1989)

A random walk on a site percolation lattice with absorbing sites is used to simulate nuclear magnetic relaxation in a porous medium. The computed relaxation is compared to a sum of exponentials with relaxation rates proportional to the pore surface-to-volume ratios. Each isolated region of the pore space is treated as a single pore rather than as a collection of connected pores. Thus, above the percolation threshold, the pore space is essentially a single large pore. For fast diffusion this sum of exponentials gives excellent agreement with the computed results. It appears that measurements in the fast-diffusion range will give only an average surface-to-volume ratio of the pore space.

I. INTRODUCTION

For some time nuclear magnetic resonance has been of interest as a means of studying the structure of porous media.[1] One approach has been to investigate the spin-orbit relaxation of proton magnetization on molecules of the pore fluid. Typically the magnetization is treated as a continuous variable. Then the longitudinal component, M, satisfies the equation[2,3]

$$\frac{\partial M}{\partial t}=D\nabla^2 M-\frac{M}{T_{1b}} \tag{1}$$

with the boundary condition

$$D\hat{\mathbf{n}}\cdot\nabla M+\rho M=0\ , \tag{2}$$

and the initial condition

$$M(\mathbf{r},0)=M_0\ . \tag{3}$$

Here D is the bulk diffusion coefficient of the pore fluid, T_{1b} is the bulk spin-lattice relaxation time, $\hat{\mathbf{n}}$ is a unit vector pointing out of the pore space, and ρ is a measure of the strength of relaxation at the surface.

These equations can be simplified by writing

$$M(\mathbf{r},t)=M_0 g(\mathbf{r},t)e^{-t/T_{1b}}\ . \tag{4}$$

Then the relaxation function $g(\mathbf{r},t)$ satisfies the diffusion equation

$$\frac{\partial g}{\partial t}=D\nabla^2 g \tag{5}$$

with the boundary condition

$$D\hat{\mathbf{n}}\cdot\nabla g+\rho g=0 \tag{6}$$

and the initial condition

$$g(\mathbf{r},t)=1\ . \tag{7}$$

Equations (5)–(7) can be solved exactly (by separation of variables) only for single pores having spherical, cylindrical, or rectangular geometry. The form of the solution depends on the pore size a. For

$$\rho a/D\ll 1 \tag{8}$$

(fast diffusion) the relaxation is very closely approximated by

$$g(\mathbf{r},t)=e^{-\nu t} \tag{9}$$

with

$$\nu=\rho S/V\ , \tag{10}$$

where S is the surface area and V the volume of the pore. If the inequality is not satisfied, the solution can still be approximated by Eq. (9), but the approximation is not as good and there is not a simple, general relation between ν and the pore geometry. It is generally assumed that g can be approximated by Eq. (9) for a pore of arbitrary shape provided the pore is "well connected." Unfortunately, "well connected" is a subjective idea that cannot be rigorously defined.

Now suppose that we have a system of isolated pores each relaxing according to Eq. (9). Then the volume average $\bar{g}(t)$ of the relaxation function is given by

$$\bar{g}(t)=\sum_i f_i e^{-\nu_i t} \tag{11}$$

where f_i is the volume fraction of pores with relaxation rate ν_i. Equivalently $\bar{g}$ can be written in the integral form[3]

$$\bar{g}(t)=\int_0^\infty P(\nu)e^{-\nu t}d\nu \tag{12}$$

where $P(\nu)$ is the probability density of ν. That is, the average relaxation function is the Laplace transform of the relaxation rate probability density. And, for fast diffusion, the relaxation rate is related to the pore size through Eq. (10). Thus the relaxation function is determined by a distribution of pore sizes.

Almost all analyses of nuclear magnetic relaxation in porous media have been based on the model described above. The material consists of isolated pores. The relaxation in each pore is dominated by a single relaxation rate. And the relaxation rate is determined by the pore surface-to-volume ratio. There have been a few attempts to treat a system composed of interconnected pores.[1,4–7] In particular Ref. 7 discusses experiments and calculations in which nuclear magnetic relaxation is related to

the total surface-to-volume ratio of the pore space. However, this reference does not consider the distribution of pore surface-to-volume ratios. Nor does it study the effect of varying ρ. Only a single value of ρ is treated.

To look at the problem in somewhat more detail I have considered a generalization of the "ant in the labyrinth" diffusion model proposed by de Gennes.[8,9] In this model the ant executes a random walk on the sites of a percolation lattice. The generalization is that when the ant attempts to step on a closed site it has a probability of being killed. The relaxation function $g(\mathbf{r},t)$ then corresponds to the probability that the ant is alive and at position $\mathbf{r}$ at time t if it initially has equal probability to be at any open site. The average relaxation function $\bar{g}(t)$ corresponds to the probability that the ant is still alive at time t.

II. THE LATTICE MODEL

We consider a hypercubic site percolation lattice in d dimensions. The sites are open with probability p and closed with probability $1-p$. An ant walks on the open sites of the lattice taking steps at equal intervals of time τ. At each step the ant steps to a neighboring open site with probability $\mu/2d, 0 \le \mu \le 1$. It steps to a neighboring closed site and is killed with probability $\gamma/2d, 0 \le \gamma \le 1$. And it remains alive at its initial site with probability

$$1-\left[1-\frac{z}{2d}\right]\mu-\frac{z}{2d}\gamma \tag{13}$$

where z is the number of neighboring closed sites. Periodic boundary conditions are used.

The percolation model cannot be compared directly with the continuum model. Equation (2) implies a smooth boundary with a well-defined normal $\hat{\mathbf{n}}$, whereas the percolation model has a rough boundary. However, we can compare the continuum model with a lattice model that is exactly as described above except for having a smooth boundary.

The relaxation function $g(\mathbf{r},t)$ in the continuum model corresponds in the lattice model to $g_n(\mathbf{r})$, the probability that an ant is alive at position $\mathbf{r}$ after n steps. The initial condition (7) corresponds to the condition that the ant initially has equal probability to be at any open site. The volume average relaxation function $\bar{g}(t)$ corresponds to $\bar{g}_n$, the probability that an ant is alive somewhere after n steps. The relation of the parameters in the two models is (see the Appendix)

$$D=\mu\epsilon^2/2d\tau\,, \tag{14}$$

and

$$\rho=\gamma\epsilon/2d\tau\,, \tag{15}$$

where ϵ is the lattice spacing. Equation (15) differs from the relation reported by Banavar and Schwartz.[1] From Eqs. (14) and (15)

$$\rho a/D=\gamma a'/\mu \tag{16}$$

and

$$\rho St/V=\gamma S'n/2dV' \tag{17}$$

where $a=a'\epsilon$, $S=S'\epsilon^{d-1}$, $V=V'\epsilon^d$, and $t=n\tau$.

III. RESULTS AND DISCUSSION

Simulations were done on 100×100 square lattices and $25\times25\times25$ cubic lattices. All simulations were done with $\mu=1$. The simulated survival probabilities $\bar{g}_n$ were compared with expansions, of the form (11), in terms of the pore surface-to-volume ratios. In Eq. (11) the surface-to-volume ratios are taken for isolated pores. Therefore, in this calculation, each isolated region of the pore space was treated as a single pore rather than as a system of connected pores. We will see below that, for small γ, this leads to a very close agreement between Eq. (11) and the simulation.

The percolation threshold p_c for square, site percolation lattices is[10] 0.592 75. Square lattices with $p=0.498$, 0.593, and 0.695 were used in this study. For cubic lattices p_c is[10] 0.3117. Cubic lattices with $p=0.204$, 0.314, and 0.401 were used. Distributions of surface-to-volume ratios for square lattices with $p=0.498$ and 0.593 are shown in Figs. 1 and 2. For $p=0.695$ almost the entire pore space was in a single large pore with $S'/V'=1.2$. Distributions of surface-to-volume ratios for cubic lattices with $p=0.204$ and 0.314 are shown in Figs. 3 and 4. For $p=0.401$ the pore space is dominated by a single pore with $S'/V'=3.4$.

Calculations of the survival probability $\bar{g}_n$ for the six lattices were made for values of γ from 0.01 to 0.9. Sample curves are shown for two dimensions ($p=0.593$) in Figs. 5 and 6 and for three dimensions ($p=0.314$) in Figs. 7 and 8. In these figures the points are for the simulated relaxations while the solid curves were obtained from Eq. (11). The curves were computed only down to $\bar{g}_n=0.001$. For $\bar{g}_n<0.001$, statistical fluctuations in the simulated results become too large. Curves for the other lattices were similar, but with some differences in details.

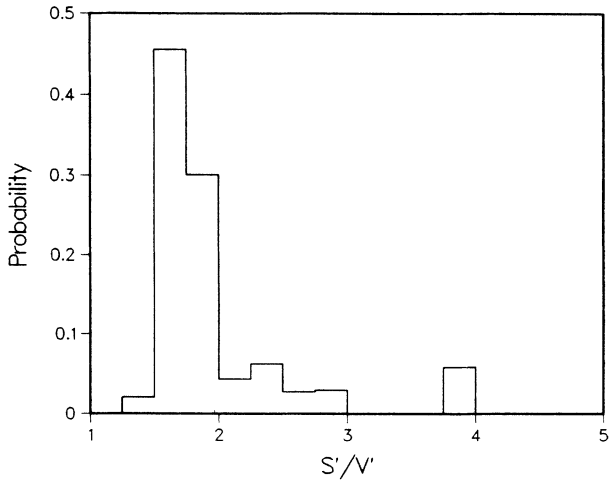

FIG. 1. Pore size distribution, square lattice, $p=0.498$.

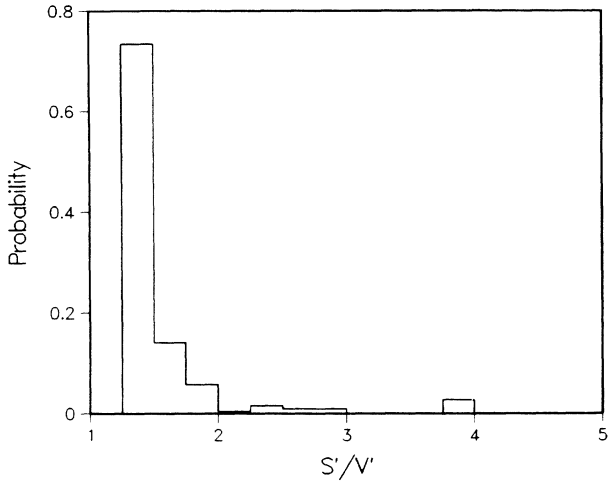

FIG. 2. Pore size distribution, square lattice, $p = 0.593$.

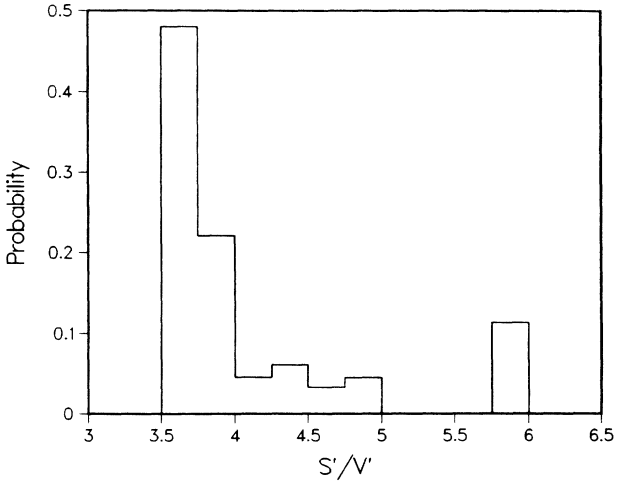

FIG. 4. Pore size distribution, cubic lattice, $p = 0.314$.

In all cases there is excellent agreement between the simulated results and Eq. (11) for small values of γ. At larger values of γ Eq. (11) deviates from the simulated results. The direction of the deviations differs in two and three dimensions. In two dimensions Eq. (11) lies below the simulated points whereas in three dimensions it lies above. As yet I have no explanation for this difference.

The simulated curves begin to deviate from Eq. (11) at a value γ_c that differs for each lattice. We expect γ_c to yield an upper limit on $\rho a/D = \gamma a'/\mu$ above which the inequality (8) is not satisfied. However it is not clear what should be used for a. For a sphere or circle a is the radius and for a cube or square it is the edge. But even for a cylinder or rectangle there are several characteristic lengths and it is not clear what combination of these should be used for a. For the highly irregular pores of a percolation lattice the situation is even more confusing.

For a rough comparison let us use a_m, the maximum pore volume-to-surface ratio. For each lattice Table I lists the site probability p, the limiting value γ_c, the maximum pore volume-to-surface ratio a'_m, the maximum pore volume V'_m, and $\gamma_c a'_m/\mu = \rho_c a_m/D$. For three dimensions the value of $\gamma_c a'_m/\mu$ seems reasonable as an upper limit on the inequality (8). For two dimensions it seems rather low. However, the correct quantity to use for a could be much larger than the volume-to-surface ratio. For a cube it is larger by a factor of 6. Thus, all that one can say is that the range of γ for which Eq. (11) agrees with the simulated results is clearly within the fast-diffusion range. Why two and three dimensions show different behavior is not yet explained.

A final interesting feature of the lattices can be observed from the data in Table I. As p increases from below to above the percolation threshold, there is a very large increase in the maximum pore volume. Over the same range of p the maximum volume-to-surface ratio changes only slightly going through a minimum at the

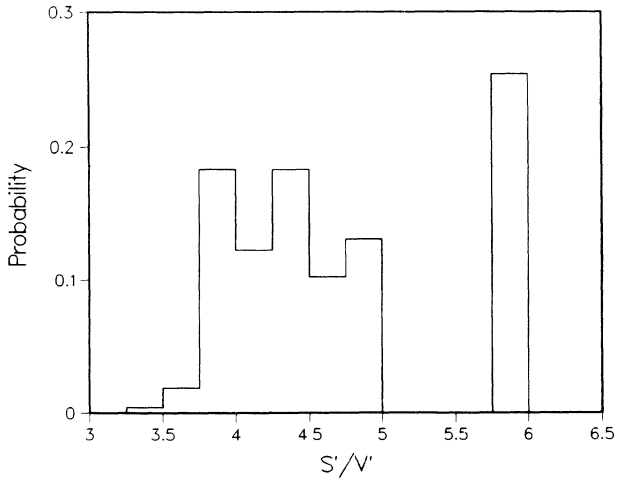

FIG. 3. Pore size distribution, cubic lattice, $p = 0.204$.

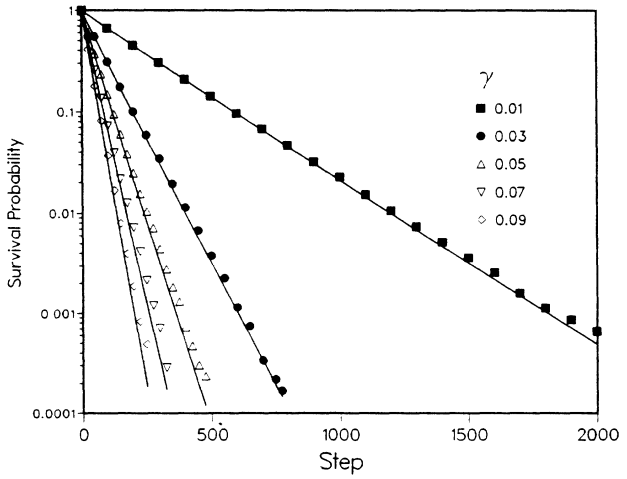

FIG. 5. Sample relaxation curves, square lattice, $p = 0.593$, small γ. Points are from computer simulations, solid lines are from Eq. (11).

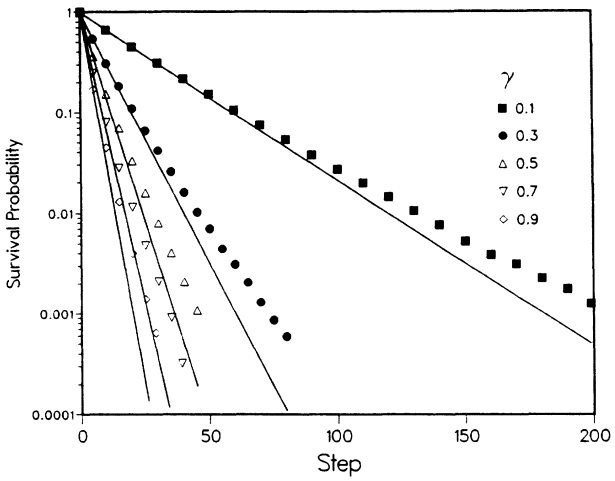

FIG. 6. Sample relaxation curves, square lattice, $p=0.593$, large γ. Points are from computer simulations, solid lines are from Eq. (11).

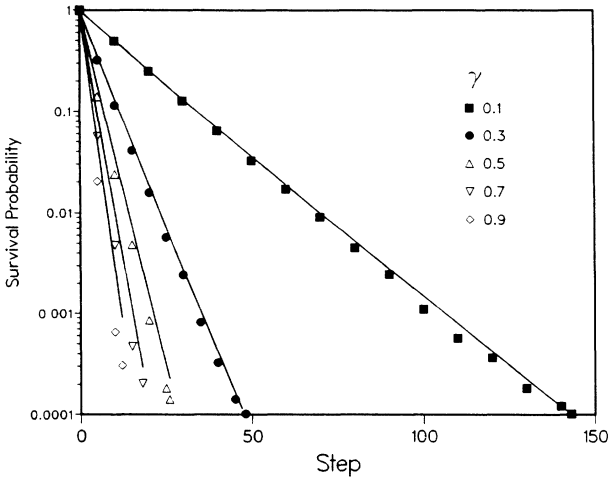

FIG. 8. Sample relaxation curves, cubic lattice, $p=0.314$, large γ. Points are from computer simulations, solid lines are from Eq. (11).

percolation threshold. This is clearly caused by the highly irregular shape of the pore space; the largest pore is fractal near the percolation threshold. The pore surfaces are larger and increase more rapidly with increasing p than would be expected for nonfractal surfaces.

In the fast-diffusion range, for lattices above the percolation threshold, the relaxation curves are exponential. The exponents are proportional to the surface-to-volume ratio of the single large pore that dominates the pore space. Below the percolation threshold there is a range of pore sizes and Eq. (11) contains several terms. Nevertheless, in the fast-diffusion range, where Eq. (11) fits the relaxation curves, these curves differ only slightly from exponentials. Within the accuracy of the calculations one cannot invert the simulated relaxation curves to obtain the distribution of surface-to-volume ratios. The most that one can obtain is an average surface-to-volume ratio for the entire pore space.

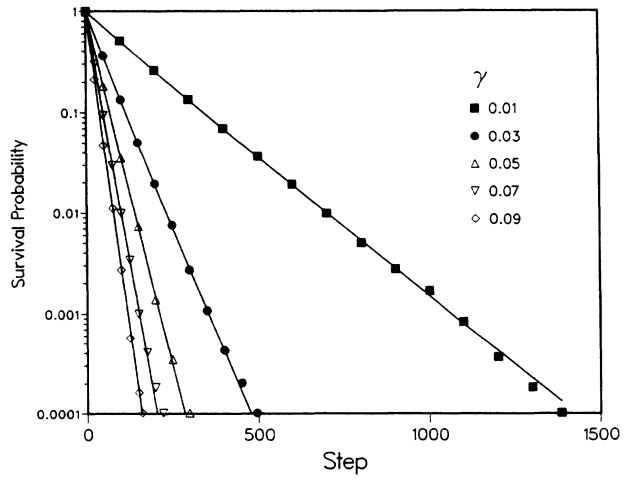

FIG. 7. Sample relaxation curves, cubic lattice, $p=0.314$, small γ. Points are from computer simulations, solid lines are from Eq. (11).

This also seems to be the situation for measurements on water filled sedimentary rock.[11,12] The measured magnetization curves differ only slightly from exponentials. Schmidt, Velasco, and Nur[11] interpreted their measured magnetization in terms of two pore sizes. But Brown[13] has argued that their data are not sufficiently accurate to distinguish between two exponentials and a single exponential. Halperin *et al.*[12] have interpreted their measured magnetization as an average over a region, which they call a diffusion cell, that is large compared to a pore size. That is, they treat the pore space as a collection of connected pores rather than as a single large pore. The results of the present paper suggest that in the fast-diffusion range it is more appropriate to treat the pore space as a single very large pore. The magnetization is determined by the surface-to-volume ratio of this pore.

To understand this, we integrate Eq. (5) over the volume of the medium; then apply Gauss's divergence theorem and Eq. (6) to obtain

$$\int \frac{\partial g(\mathbf{r},t)}{\partial t} dV = -\rho \oint g(\mathbf{r},t) dS \ . \tag{18}$$

TABLE I. Characteristic parameters of the percolation lattices.

p	γ_c	a'_m	V'_m	$\gamma_c a'_m/\mu$
0.498[a]	0.07	0.772	520	0.05
0.593[a]	0.05	0.730	4150	0.04
0.695[a]	0.03	0.845	6840	0.02
0.204[b]	0.3	0.295	49	0.09
0.314[b]	0.4	0.283	1050	0.11
0.401[b]	0.6	0.293	5740	0.18

[a]Two dimensions.
[b]Three dimensions.

Because the boundary of the region of integration is fixed, the time derivative can be taken out of the integral. This yields

$$\frac{d\bar{g}(t)}{dt} = -\frac{\rho}{V}\oint g(\mathbf{r},t)dS \ . \tag{19}$$

Now if g is uniform over the medium, i.e., $g(\mathbf{r},t)=\bar{g}(t)$, it can be taken out of the integral yielding Eqs. (9) and (10). The results of the present study suggest that this will always be the case, regardless of the shape of the pore, provided (a) ρ/D is small enough and (b) the pore is connected. Note that the pore need not be "well connected." The poorer the connections the smaller ρ/D will have to be to have g uniform throughout the pore.

Thus we see that in the fast-diffusion range each isolated region of the pore space relaxes uniformly with a rate that is proportional to its surface-to-volume ratio. Indeed this can be taken as the definition of the fast-diffusion range. In a material, such as sedimentary rock, in which most of the pore space consists of a single interconnected region, the relaxation is exponential. And the relaxation rate is proportional to the total surface-to-volume ratio of the pore space. No further information about the pore geometry can be obtained from NMR measurements in the fast-diffusion range. However, the relaxation for slow diffusion does appear to depend on the details of the pore geometry. Further investigation is necessary to determine what information can be obtained from measurements in this range.

APPENDIX: DERIVATION OF EQS. (14) AND (15)

We consider a hypercubic lattice in d dimensions. First consider a site at the edge of the pore space which has one closed neighbor and $2d-1$ open neighbors. Let x_1 be the coordinate through the closed site with the positive direction toward the closed site, i.e., pointing out of the pore space. Then the probability $g_n(x_1,\ldots,x_d)$ that an ant is at the site after n steps satisfies the equation

$$g_{n+1}(x_1,\ldots,x_d)=\frac{\mu}{2d}\sum_{k=2}^{d}[g_n(x_1,\ldots,x_k+\epsilon,\ldots,x_d)+g_n(x_1,\ldots,x_k-\epsilon,\ldots,x_d)]$$
$$+\frac{\mu}{2d}g_n(x_1-\epsilon,\ldots,x_d)+\left[1-\left[1-\frac{1}{2d}\right]\mu-\frac{\gamma}{2d}\right]g_n(x_1,\ldots,x_d) \ . \tag{A1}$$

Subtract $g_n(x_1,\ldots,x_d)$ from both sides of this equation, multiply by ϵ/τ, and rearrange terms to obtain

$$\epsilon\frac{g_{n+1}(x_1,\ldots,x_d)-g_n(x_1,\ldots,x_d)}{\tau}$$
$$=\frac{\mu\epsilon^3}{2d\tau}\sum_{k=2}^{d}\frac{g_n(x_1,\ldots,x_k+\epsilon,\ldots,x_d)-2g_n(x_1,\ldots,x_k,\ldots,x_d)+g_n(x_1,\ldots,x_k-\epsilon,\ldots,x_d)}{\epsilon^2}$$
$$+\frac{\mu\epsilon^2}{2d\tau}\frac{g_n(x_1-\epsilon,\ldots,x_d)-g_n(x_1,\ldots,x_d)}{\epsilon}-\frac{\gamma\epsilon}{2d\tau}g_n(x_1,\ldots,x_d) \ . \tag{A2}$$

Now take the limit $\epsilon\to 0$, $\tau\to 0$, $\gamma\to 0$, while $\mu\epsilon^2/2d\tau=D$, and $\gamma\epsilon/2d\tau=\rho$. With $g_n(x_1,\ldots,x_d)\to g(x_1,\ldots,x_d,t)$, Eq. (A2) becomes

$$\epsilon\frac{\partial g}{\partial t}=\epsilon D\sum_{k=2}^{d}\frac{\partial^2 g}{\partial x_k^2}-D\frac{\partial g}{\partial x_1}-\rho g \ . \tag{A3}$$

In the limit $\epsilon\to 0$ the left side and the first term on the right side of Eq. (A3) vanish. If the boundary surface is smooth with a well-defined normal $\hat{\mathbf{n}}$ then $\partial g/\partial x_1=\hat{\mathbf{n}}\cdot\nabla g$ and the last two terms of Eq. (A3) give Eqs. (14) and (15).

The limit $\gamma\to 0$ might seem to imply that Eq. (15) is valid only in the fast-diffusion range. But this is not the case. Whether the system is in fast or slow diffusion is determined by the value of $\rho/D=\gamma/\mu\epsilon$ which remains fixed as the limit is taken. In the relation between ρ and γ given by Banavar and Schwartz,[1] γ in Eq. (15) is replaced by $\gamma/(1-\gamma)$. This is the same as Eq. (15) in the limit, but not otherwise.

If one goes through the previous argument for a point that has no closed neighbors, one obtains Eq. (A3) except that the sum is over all coordinates and the last two terms on the right do not appear. Then on cancelling ϵ and taking the limit one obtains Eq. (5) with Eq. (14).

For a site with more than one closed neighbor one again obtains Eq. (A3) but with more first and fewer second derivative terms. Taking the limit leads to Eq. (6) if the surface has a well-defined normal. In this case, however, the normal does not lie along one of the coordinate axes.

[1]J. R. Banavar and L. M. Schwartz, in *Molecular Dynamics in Restricted Geometries,* edited by J. Klafter and J. M. Drake (Wiley, New York, 1989).
[2]K. R. Brownstein and C. E. Tarr, Phys. Rev. A **19**, 2446 (1979).
[3]M. H. Cohen and K. S. Mendelson, J. Appl. Phys. **53**, 1127 (1982).
[4]K. S. Mendelson, J. Electrochem. Soc. **133**, 631 (1986).
[5]K. S. Mendelson, Physica **A157**, 489 (1989).

[6]J. R. Banavar and L. M. Schwartz, Phys. Rev. Lett. **58**, 1411 (1987).

[7]C. Straley, A. Matteson, S. Feng, L. M. Schwartz, W. E. Kenyon, and J. R. Banavar, Appl. Phys. Lett. **51**, 1146 (1987).

[8]P. G. deGennes, La Recherche **7**, 919 (1976).

[9]C. D. Mitescu, H. Ottavi, and J. Roussenq, in *Electrical Transport and Optical Properties of Inhomogeneous Media (Ohio State University, 1977),* Proceedings of the First Conference on the Electrical Transport and Optical Properties of Inhomogeneous Media, AIP Conf. Proc. No. 40, edited by J. C. Garland and D. B. Tanner (AIP, New York, 1978), p. 377.

[10]D. Stauffer, *Introduction to Percolation Theory* (Taylor and Francis, London, 1985), p. 17.

[11]E. J. Schmidt, K. K. Velasco, and A. M. Nur, J. Appl. Phys. **59**, 2788 (1986).

[12]W. P. Halperin, F. D'Orazio, S. Bhattacharja, and J. C. Tarczon, in *Molecular Dynamics in Restricted Geometries,* edited by J. Klafter and J. M. Drake (Wiley, New York, 1989).

[13]R. J. S. Brown, J. Appl. Phys. **63**, 1244 (1988).